

archives
of thermodynamics

Vol. 41(2020), No. 1, 245–263

DOI: 10.24425/ather.2020.132957

Optimisation of the performance of a pyrolysis reactor for G50 chips

ALOK DHAUNDIYAL ^{*a}
SURAJ SINGH ^b

^a Institute of Process Engineering, Szent István University, Páter Károly 1., 2100, Gödöllő, Hungary

^b Department of Mathematics, Statistics and Computer Science, Govind Ballabh Pant University of Agriculture and Technology, Pantnagar, 263145, Uttarakhand, India

Abstract The aim of any industrial plant, which is dealing in the energy sector, is to maximise the revenue generation at the lowest production cost. It can be carried out either by optimizing the manpower or by improving the performance index of the overall unit. This paper focuses on the optimisation of a biomass power plant which is powered by G50 hardwood chips (Austrian standard for biomass chips). The experiments are conducted at different operating conditions. The overall effect of the enhanced abilities of a reactor on the power generation is examined. The output enthalpy of a generated gas, the gas yield of a reactor and the driving mechanism of the pyrolysis are examined in this analysis. The thermal efficiency of the plant is found to vary from 44 to 47% at 400 °C, whereas it is 44 to 48% for running the same unit at 600 °C. The transient thermal condition is solved with the help of the lumped capacitance method. The thermal efficiency of the same design, within the constraint limit, is enhanced by 5.5%, whereas the enthalpy of the produced gas is magnified by 49.49% through nonlinear optimisation. The temperature of biomass should be homogenous, and the ramping rate must be very high. The 16% rise in temperature of the reactor is required to reduce the mass yield by 20.17%. The gas yield of the reactor is increased by up to 85%. The thermal assessment indicates that the bed

*Corresponding Author. Email: alok.dext@hotmail.com

is thermally thin, thus the exterior heat transfer rate is a deciding factor of the pyrolysis in the reactor.

Keywords: Biomass; Thermal analysis; Pyrolysis; Gas yield; Performance index

Nomenclature

A_s	–	surface area of the bed, m ²
A_s	–	cross-sectional area, m ²
Bi	–	Biot number
C_R	–	residual fraction of unburnt carbon, %
C_{ab}	–	oxidised Carbon fraction, %
C_f	–	fraction of carbon in dry gas, %
C_{pa}	–	specific heat of ash, kJ/kgK
C_{pg}	–	specific heat of gas, kJ/kgK
Fo	–	Fourier number
ΔH_g	–	enthalpy of gas, kJ/kg
h	–	heat transfer coefficient, kW/m ² K
k	–	thermal diffusivity, m ² /s
L_c	–	characteristic length, m
M_c	–	residual mass of carbon, g
Q_1	–	energy loss due to unburnt carbon residue, kJ/kg
Q_2	–	energy loss while formation of carbon monoxide (CO), kJ/kg
Q_3	–	energy loss due to moisture in fuel, kJ/kg
Q_4	–	energy loss due to exhaust gas, kJ/kg
Q_5	–	energy loss due to hydrogen in fuel, kJ/kg
Q_6	–	energy loss due to refuse, kJ/kg
Q_7	–	energy gain by the bed due to conduction, kJ/kg
Q_8	–	energy loss through rockwool insulation, kJ/kg
w_f	–	biomass consumption rate, kg/s
w_g	–	gas flow rate, kg/s
W_d	–	dry gas per kg of fuel, kg
T_g	–	maximum temperature, °C
T_f	–	initial temperature °C
T_0	–	ambient temperature, °C
T_e	–	average temperature, °C
Q_i	–	various heat losses, kJ/kg
r	–	radius of insulation packing, m
T	–	temperature at arbitrary time, °C
T_i	–	initial temperature, °C
$T_{A,B,C,D}$	–	average temperature at location marked by subscript A, B, C, D, °C
t	–	time, s
V_b	–	volume of bed, m ³

Greek symbols

η_{th}	–	thermal efficiency
ε	–	voidage
ρ_b	–	density of bed, kg/m ³

1 Introduction

Problems with the conventional energy system are not only connected to global warming but also have some environmental concerns such as air pollution, acid precipitation, ozone depletion, emission of the radioactive substance and the forest infernos. These issues can be countered if the energy devices become more efficient and provide a sustainable energy future. The cost-effective productivity with lower greenhouse gases (GHG) emission is the desirable goal of any power plant, however, it increases the primary cost of the plant, but the cost can be recovered through suitable operative conditions. For such complex bodies, optimisation scheme provides a suitable platform for the valorisation of the whole power station in terms of efficiency, plant load factor (PLF), use factor and the net heat rate (NHR) of a power plant. Therefore, various alternative sources need to be explored and the pyrolysis process is one of them. Thermochemical conversion of biomass and urban wastes for upgrading energy, in the context of material handling (gases, liquid, and charcoal), has been becoming very promising for the last decade [1–4].

The end products of pyrolysis can be commercially lucrative, but without enhancing the ability of the power plant, it is impossible to meet the objective. The process conditions and the feedstock properties are very useful to comprehend the product distribution of the chemical/power plants. The pyrolysis of lignocellulose is not only a methodology of solid fuel conversion but also a primal part of the gasification and the combustion processes. The product yield is based upon the heating regime, pyrolysis mechanism, the residence time of volatile, particle size and the direction of flow of heat across the grains. The slow-conventional pyrolysis is applied to produce high charcoal yield which can be boosted up to 50% by operating at elevated pressures in a stagnant gaseous environment [5]. The pre-treatment of biomass may also alter the yield of products, such as the effect of torrefaction on the flash pyrolysis. The flash pyrolysis (1000 °C/min) is associated with a high reduction in the solid residual yield, but the same heating regime gets altered if the biomass gets pre-treated before pyrolysis. The torrefaction process enhances depolymerisation and cross-linking. Thus, the char yield gets promoted even in the fast pyrolysis condition [6,7]. The objective of pyrolysis is to maximise either gas or liquid yield, which mainly depends on temperature and residence time. A fluid-bed reactor encourages the gas production if the operating temperature is higher than 920 K and the residence time of about 1 s [8], whereas the characteristics of the re-

actor for high liquid yields operate at the temperature range of 670–920 K and relatively small residence times. This methodology can produce the enriched quality of biofuel at the cost of low fuel feed rate. The objective of this technology is to generate high calorific bio-oil or gas by replacing conventional fossil fuels.

The performance of different pyrolysis reactors can be predicted through the specific model, however, the size of the particle may demarcate the chemical and the physical processes [9]. The effect of internal and external heat transfer and pyrolysis kinetics on the conversion process through the introduction of characteristic numbers has been reported in the literature [10–14]. The internal pyrolysis number, the ratio of the reaction time to the conduction time, is an index of assessing the intraparticle processes. The variation of pyrolysis and Biot number (Bi) provides sufficient information about whether the process is controlled through internal heat transfer or not. Although, for defining the different regimes of solid pyrolysis (when both the numbers are less than one), the external pyrolysis number is required to know the relative importance between kinetic and internal transfer. If $Bi < 1$, the regime has been recognised as a ‘thermally thin’. On the other hand, for $Bi > 1$, the regime has been identified as a ‘thermally thick’ [10,15]. The internal heat transfer is relatively slow as compared with external heat transfer, and a substantial thermal gradient is set across intraparticle, in the latter case. The energy analysis of a reactor at different sections of the reactor or different operating conditions provides an insight into the energy management of the plant. The major losses mainly occur inside the reactor; thus, this study emphasises on minimising the energy losses and valorisation of the produced gas through the computational interface. The energy assessment is used to carry out the thermodynamic evaluation of power at different working conditions [16–18]. Many researchers [16–18] have suggested that the thermodynamic performance of a process is best evaluated with the qualitative assessment of a plant. Application of thermal assessment has included perusal of coal-fired electricity generation using conventional [19–22], fluidized-bed combustion and combined cycle [23–26]. The investigation is based on the thermodynamics of energy production and optimisation of its performance. The computational interface is employed to pinpoint the locations where the significant losses occurred during thermochemical conversion. To better understand the role of key design factor, a performance evaluation of a pilot size unit is conducted for different conditions.

2 Material and methods

2.1 Thermal analysis

Thermoanalytical schemes have been mainly used to examine the thermal behaviour of conventional fuel [27,28] and biofuels [29]. The thermal efficiency of a pilot plant (Fig. 1) can be determined through the thermal behaviour of biomass, therefore it is necessary to improve the decomposition rate so that the enthalpy of gas is optimised without causing the excessive pressure drops across the reactor. The slugging and bubbling of bed influence the pressure distribution and so as the exergy destruction. However, in the real process, exergy is always destroyed due to inherent irreversibility, but it can be minimised by optimising the certain parameters associated with the thermochemical process.

A thermodynamic study of a reactor is conducted at an operating range of 400 °C and 600 °C. The pressure of a gas varies from 0.05 kPa to 42.5 kPa at 400 °C, whereas it is 0.135 kPa to 1.34 kPa at 600 °C. The thermal assessment is carried for both cases and on the basis of output data, an interior point algorithm has been designed in the Matlab to optimise thermal parameters of the reactor. Both the linear and non-linear programming is used to enhance the performance index of a pilot size unit. A sensitivity analysis is done to determine the fluctuation of the objective function with an operating condition so that the best values can be obtained within the given constraints. Finally, some thermal losses and the conversion calculated. During working of testing rig there are some losses encountered, which are evaluated through the following expressions [30].

Energy loss due to unburnt carbon residue

$$Q_1 = 33917(C - C_{ab}) \text{ kJ/kg} , \quad (1)$$

where, C is the carbon content of fuel and C_{ab} is the oxidised carbon fraction.

Energy loss during formation of carbon monoxide (CO)

$$Q_2 = 10100W_d [28\text{CO}/(28\text{CO} + 16\text{CH}_4 + 44\text{CO}_2 + 2\text{H}_2 + 28\text{N}_2)] \text{ kJ/kg}, \quad (2)$$

where W_d represents the mass of dry gas per kg of biomass.

Energy loss due to moisture in fuel

$$Q_3 = M (4.2 (100 - T_f) + 2256.8 + 2.09 (T_g - 100)) \text{ kJ/kg} . \quad (3)$$

Here, T_f is the initial temperature at time $t = 0$ and T_g denotes the final temperature at different sections of the reactor.

Energy loss due to exhaust gas

$$Q_4 = W_d C_{pg} (T_e - T_0) , \quad (4)$$

where T_e is the average temperature across the bed and T_0 is the ambient temperature (288 K).

Energy loss due to hydrogen in fuel

$$Q_5 = 9H [4.2 (100 - T_f) + 2256.8 + 2.09 (T_g - 100)] . \quad (5)$$

Energy loss due to refuse

$$Q_6 = [(C - C_{ab}) + A] C_{pa} (T_g - T_0) , \quad (6)$$

where A is the residual ash content, C_{pa} is the specific heat of ash.

Energy gain by the bed due to conduction- unsteady-state (lumped system analysis)

$$Q_7 = \rho_b V_b \frac{dT}{dt} = h A_s (T - T_0) , \quad (7)$$

where ρ_b and V_b denote the density and the volume of bed, respectively [31].

For the transient condition, the temperature distribution is given by

$$\theta = \theta_0 \exp \left(-\frac{h A_s t}{\rho_b V_b} \right) \text{ or } \theta = \theta_0 \exp^{(-\text{Bi Fo})} .$$

Here the Biot (Bi) and the Fournier (Fo) numbers signify the temperature distribution and degree of penetration of heat across the bed respectively, and A_s represents the surface area of bed, t denotes the time and h is the heat transfer coefficient:

$$\text{Bi} = \frac{h L_c}{k} , \quad \text{Fo} = \frac{\alpha t}{L_c^2} ,$$

where $\theta = T - T_0$ and $\theta_0 = T_i - T_0$, T – temperature at time t . Then

$$Q_7 = \frac{h\theta_0 A_s \left(e^{\text{Bi} \text{Fo}} \right)}{w_f} ; , \quad (8)$$

where w_f is the biomass consumption rate.

Energy loss through rockwool insulation

$$Q_8 = \frac{\frac{(T_e - T_0)}{\sum_{n=1}^{n=k} \frac{1}{k_{n-1}} \ln \left(\frac{r_n}{r_{n-1}} \right)}}{w_f} , \quad (9)$$

where r denotes the radius of boundary that surrounded the bed, k is the thermal conductivity of the bed.

The summation of the total loss is estimated by

$$\sum Q_{loss} = Q_1 + Q_2 + Q_3 + Q_4 + Q_5 + Q_6 - Q_7 + Q_8 . \quad (10)$$

The actual dry gas per kg of fuel and the theoretical yield of gas are computed as:

$$W_d = \frac{C_{ab} [44\text{CO}_2 + 28\text{CO} + 2\text{H}_2 + 16\text{CH}_4]}{12[\text{CO} + \text{CO}_2 + \text{CH}_4]} / \text{per kg of fuel} , \quad (11)$$

$$W_{th} = \frac{C [44\text{CO}_2 + 28\text{CO} + 2\text{H}_2 + 16\text{CH}_4]}{12[\text{CO} + \text{CO}_2 + \text{CH}_4]} / \text{per kg of fuel} . \quad (12)$$

2.2 Experimental installation

The tests have been conducted at the National Agriculture Research and Innovation Centre, Hungary. The raw material, the G50 hardwood (Acacia) chips, has been used in the pyrolysis unit (Fig. 1). The physicochemical characteristic of the raw material is determined through physical and chemical analysers. The intensive (T , P) and the extensive (m) properties are determined by incorporating the different kind of sensors (Fig. 2.) around the periphery of the testing rig. The temperature sensors are placed at equidistance from each other, that is 80 mm apart, whereas the pressure and the weight sensors are retrofitted near the base of the unit. The ‘K’ type (nickel-chromium/nickel-alumel) thermocouple is used for this study.

The purge gas (N_2) is allowed to flow at the volumetric rate of 0.7 L/s and at the outlet pressure of 150 kPa. The maximum pressure at the inlet of the Nitrogen gas cylinder is 5000 kPa. The weight sensor is protected from getting damaged by the insulating cap. All these sensors are connected to the PC *via* the multioperating data logger. The indirect heating of the reactor is provided by a 2 kW heating element (Hertz). The grid material is manufactured of 0.7 mm stainless steel, while the Rockwool covering of 50 mm is provided to prevent the heat losses around the periphery of the pyrolysis reactor. The core of the pyrolysis chamber is formed of 1.5 mm thick welded carbon steel. The inner and the surface diameters of the reactor are 110 mm and 210 mm, respectively. There is an aluminium foil wrapped around the insulating material (Rockwool) to protect it from getting damaged. The thickness of insulating material is 50 mm. The raw as well as the carbonised part of the G50 chips are illustrated in Fig. 3.

The elemental composition of the raw material is measured by a CHNO-S analyser (Vario MACRO cube). The tungsten oxide (WO_2) powder (Wolfram, Germany) is mixed with the sample to facilitate the pre-combustion of the sample. Firstly, the analyser is calibrated for birch leaves so that it can be ensured whether the device is properly working or not. The analyser is heated up to 1200 °C for 30 min, and once it reaches the pre-combustion required for the given material, the capsule form of the sample is fed into the rotating disk. The flow rate of oxygen maintains the catalytic combustion, whereas helium gas is used as a carrier gas for the products of combustion. The products of combustion are latterly separated into its constituents through trap chromatography. The halogen content is detected through a similar unit, which is equipped with an infrared detector (IR). The calorific value of hardwood is obtained using the bomb calorimeter at the constant volume. The physicochemical characteristic of hardwood is shown in Tab. 1. The ash-melting point of hardwood is measured by making an ash mould of 1.5 cm \times 1 cm. The mould is kept inside the ash melting furnace, and the temperature gets increased with respect to time. The ash of a material passes through the five major temperature zones: sintering temperature, deformation temperature, sphere temperature, hemisphere temperature and the flow temperature. Once the sharp corners of mould are getting filleted, it implies the ash material is at a verge to enter the plasticity zone. The optical bench used for this purpose is designed by the Hesse Instrument.

Table 1: The physiochemical composition of hardwood (acacia).

C (%)	H (%)	N (%)	O (%)	S (%)	Cl (%)	Ash (%)	*HCV (MJ/kg)	**NCV (MJ/kg)	Ash melting point (°C)
50.030	5.849	0.075	42.947	0.061	0.002	1.037	19.976	18.700	1973

*High calorific value ** Net calorific value

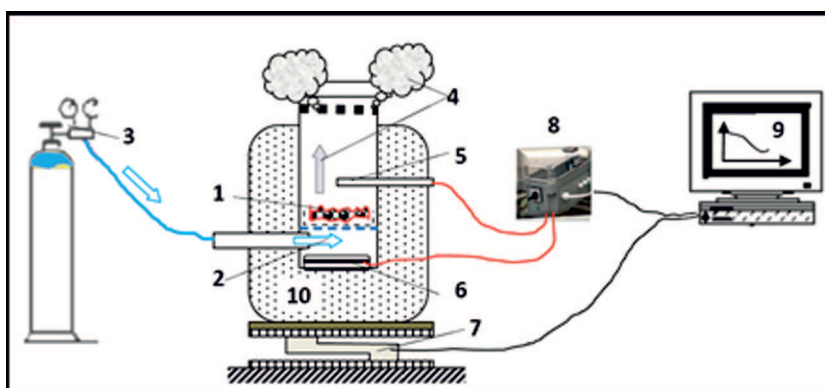
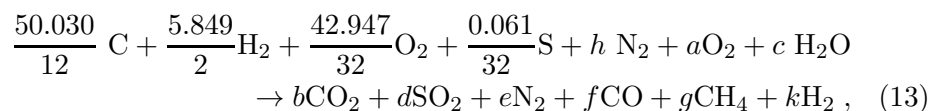


Figure 1: Schematic diagram of a pyrolysis unit: 1 – grate, 2 – nozzle, 3 – regulating valve, 4 – pyrolysis gas, 5 – temperature sensor (nickel-chromium/ nickel-alumel), 6 – pressure sensor, 7 – mass sensor, 8 – data logger, 9 – processing unit, 10 – mineral wool insulator.

3 Results and discussion

The analysis of reactor is based on the thermal conversion of fuel into the gaseous products. The different operating conditions are used to evaluate the overall enthalpy of the system. The objective functions alongside with linear as well as non-linear inequalities are optimised through the interior-point algorithm. Matlab R2015b has been used for optimising the performance of the reactor. The pyrolysis reaction is given by



where symbols $a-k$ are stoichiometric reaction coefficient. It is observed having seen a stoichiometric ratio (chemically correct ratio of air and fuel) of the system that the pyrolysis is relatively improved through optimisation,

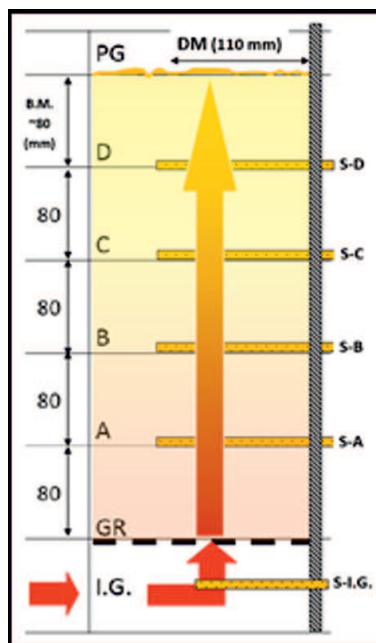


Figure 2: Location of the sensors in a pyrolysis unit: A, B, C and D – location of temperature sensor, S-I-G – mass sensor, GR – grid sheet.



(a)

(b)

Figure 3: The G50 hardwood chips before and after pyrolysis: (a) – the raw material, (b) – biochar.

thus the energy losses during the release of volatile gases have been curtailed to a greater extent by the adopted scheme. The fraction of oxygen in the products of pyrolysis is relatively increased after optimisation, nevertheless, the change in the oxygen proportion as compared to carbon and hydrogen is relatively low. The pictorial representation of pyrolysis is depicted through

the ternary diagram (Fig. 4). The diagram is divided into four zones (I, II, III, and IV). The first and second zone show the spatial arrangement of fuel and the product of combustion respectively; whereas zone III and zone IV denote the gaseous products obtained after decomposition of hardwood chips. It demarcates the limits of the thermochemical and combustion processes. The gas yield (CO, CO₂, CH₄, H₂) can be seen through the projection lines. There is nearly a 6% increase in the gas yield obtained by optimising the performance of the reactor. On the other hand, the oxidised fraction of carbon also rises by 4.8%. But the relative increase is within the given operational range.

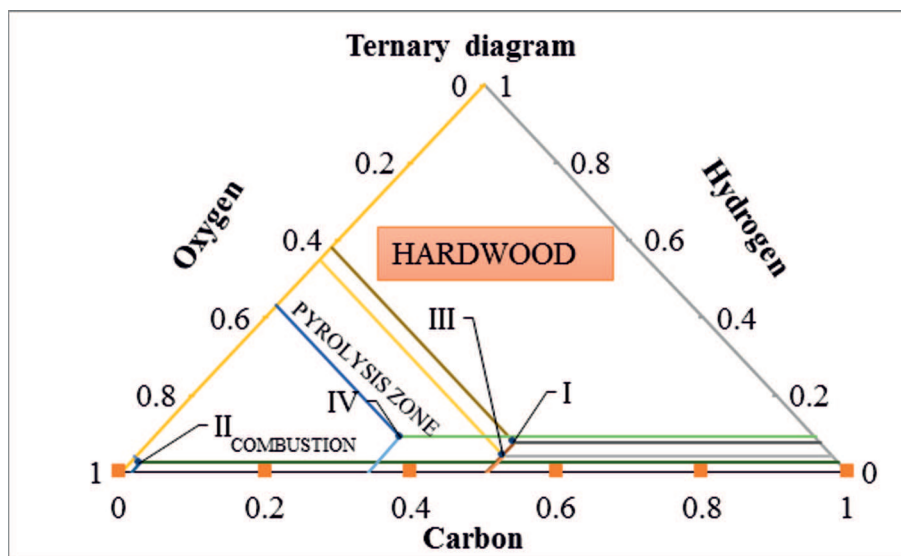


Figure 4: Ternary diagram for hardwood: I – reactant side, II – theoretical combustion, III – pyrolysis gas composition, IV – pyrolysis gas composition at optimised condition.

The parametric information of gas and fuel is shown in Tab. 4. One more thing is also highlighted through this study that it is necessary that the flow rate of gas should be relatively small as compared to the fuel consumption rate so that the pressure drop during elutriation can be minimised, however decreasing the fuel consumption rate beyond the permissible range is also not beneficial, as it affects the regimes of solid pyrolysis via altering the heat transfer mechanism among intraparticle of the bed.

The temperature distribution pattern must be quasi-isothermal near the grid of the reactor since it is necessary to minimise the exergy loss

Table 2: Actual stoichiometric reaction coefficient.

Operating condition	<i>a</i>	<i>b</i>	<i>c</i>	<i>d</i>	<i>e</i>	<i>f</i>	<i>g</i>	<i>k</i>	<i>h</i>
Optimised	0.00038	1.860	2.620	0.0019	0.0211	1.590	0.708	4.130	0.0013
400 °C	1.6012	2.250	0.430	0.0019	6.0260	1.790	0.121	3.220	6.020

Table 3: Temperature distribution across the reactor.

C_{pa}	C_{pg}	Biot number	T_g (°C)	Average temperature across different cross-section (°C)			
				T_A	T_B	T_C	T_D
1.049	2.024	0.028	463.56	454.50	355.100	325.46	299.27
1.890	1.222		400	341.27	272.42	230.94	212.72

Table 4: Gas composition (volume basis).

Operating condition	CO ₂	CO	H ₂	CH ₄	N ₂	W_d	W_{th}	Gas yield	C_{ab}	w_f	w_g
	(%)	(%)	(%)	(%)	(%)			(%)		(kg/s)	(kg/s)
463.56 °C	22.455	19.25	49.76	8.23	0.0029	1.26	1.475	85.42%	0.43	0.000313	0.0013
400-600 °C	12.2	14.3	19.9	1.8	51.8	1.21	1.489	81.22%	0.41	0.000210	0.0023

during the thermochemical conversion of the fuel. The drastic variation in thermal history affects the pathway of pyrolysis reactions. The excessive mass transfer increases tar yield, which is highly unfavourable for electricity generation through the spark-ignition (SI) engine. The structural composition of biomass is also very important to affect the yield of pyrolysis. The hardwoods comprise nearly 40–50% of cellulose, so the overall process is guided by decomposition of it. The pyrolysis of cellulose takes place over the temperature range of 280 °C to 500 °C, thus the products of decomposition are predominately the volatile fraction of biomass. The excessive increase in the temperature beyond 320 °C affects the decomposition rate of lignin and so as the residual mass fraction of carbon, which is illustrated in Tab. 6. Through the lumped heat analysis, it is found that the system

Table 5: The heat losses across different sections of a reactor.

Q_i (kJ/kg)	A			B		
	463.56 (°C)	400 (°C)	600 (°C)	463.56 (°C)	400 (°C)	600 (°C)
Q_1	2408.21	2964.34	2408.11	2408.11	2964.34	2408.11
Q_2	4979.24	4952.50	5059.71	4952.50	4952.50	5059.71
Q_3	257.31	240.05	250	228.71	228.71	241.80
Q_4	1220.89	1196.17	1519.29	943.76	943.76	1331.21
Q_5	1627.19	1603.62	1666.56	1527.87	1527.87	1612.05
Q_6	91.77	65.91	158.32	65.91	65.91	158.32
$-Q_7$	73.44	6.21	5.58	8.72	6.55	8.72
Q_8	60.86	110.33	36.35	63.70	87.05	63.70
$\sum Q_i$	10559.31	11128.62	11092.75	10169.78	10765.07	10866.17
ΔH_g [kJ/kg]	2267.24	648.76	1515.736	2361.51	680.30	10866.17

Q_i (kJ/kg)	C			D		
	463.56 (°C)	400 (°C)	600 (°C)	463.56 (°C)	400 (°C)	600 (°C)
Q_1	2408.11	2964.34	2408.11	2408.11	2964.34	2408.11
Q_2	4952.50	4952.50	5059.71	4952.50	4952.50	5059.71
Q_3	221.88	221.88	224.66	218.88	218.88	223.22
Q_4	791.68	791.68	936.77	724.89	724.89	902.78
Q_5	1482.23	1482.23	1497.74	1462.19	1462.19	1488.17
Q_6	65.91	65.91	158.32	65.91	65.91	158.32
$-Q_7$	5.03	5.03	4.14	6.08	5.58	6.08
Q_8	67.24	73.02	67.24	66.86	66.86	86.40
$\sum Q_i$	9972.02	10547.33	10348.40	9882.13	10451.44	10320.62
ΔH_g [kJ/kg]	2408.65	700.00	10348.40	2452.89	717.83	10320.62

is ‘thermally thin’, and the pyrolysis process is guided by the external heat transfer rate alone. The benefit of the thermally thin system is more homogenous carbonisation than that of ‘thermally thick’ regime [12], so the chances of getting the optimised gas yield increases, which is clearly visible in Tab. 4. The 16% rise in temperature scale, which does not deviate much from the average base temperature (TA), is required to improve the holistic performance of the reactor. But it merely depends on the objective set for the given reactor. The rapid heating rate encourages mass transfer

Table 6: Parameters related to the performance index of a reactor.

Operating condition	$\sum \overline{Q_{loss}}$ (kJ/kg)	$\overline{\Delta H_g}$ (kJ/kg)	η_{th} (%)	Carbon conversion efficiency (%)	Reactor characteristic			
					C_f (%)	W_R (g)	C_R (%)	M_c (g)
400 °C	10723.11	686.72	46.32	67	33	97.71	89	86.96
600 °C	10656.98	1587.02	46.64	67	33	78.00	86	67.08
Optimised	10145.80	2372.50	49.21	68	34	81.65	87	71.03

along with pyrolysis and char inhibition reactions to reduce the char yield [32]. The temperature gradient between the two sections is relatively small as compared to the experimental condition, which is also one of the main reasons for decreasing of entropy generation and the overall thermal loss gets minimised. The calculated thermal losses across the pyrolysis reactor are tabulated in Tab. 5. There is a 5% decrease in thermal losses at the base section of the reactor with respect to 400 °C, whereas it is nearly 5.5% for other sections (B, C, and D) of the reactor. The areas pinpointed by an interior point algorithm are the carbon conversion efficiency and the lumped heat capacitance of a reactor. The energy gain through the heating element must be very efficient to improve the thermal efficiency of the power plant. How efficiently the external heat transfer is carried out in a ‘thermally thin’ system is the most significant aspect of the power plant as it governs kinetics of pyrolysis. The overall performance of a reactor on an average basis is computed in Tab. 6.

The positive benchmark of this study is observed while doing the non-linear optimisation of enthalpy of gas so that the gas, which is being used for thermal or other power applications, improves the overall efficiency of a power plant. The enthalpy of the gas increases by 49% whereas it is not necessary that the elevation of temperature boosts-up the gas yield. The most vital part of the analysis is the minimisation or maximisation of fluid and thermal parameters so that the overall effects of them on a system improves the exergy of the power plant. In the practical situation, it is very difficult to control the heating profile of a system as various endothermic as well as exothermic reaction influence the overall heat of reaction, especially in the case of thermochemical conversion where oxygen content is very low

and the redox reaction of Boudouard affects the energy balance of a system. It influences at elevated is relatively high, and moreover, insufficient oxygen in a flame front also escalate the energy crisis during the conversion process. But the latter one usually occurs at 1127 °C when oxygen supply is hindered by the formation of CO. The thermogravimetric behaviour of G50 chips is shown in Fig. 5. The industrial reactor works on the varying heating rate; therefore, it might not be correct to correlate shifting of the mass-loss curve due to the limitation of heat-transfer [33], or inability of a system to hold an enormous thermal energy, or when the pyrolysis number is high. As it is computed that the carbon fraction in the refuse is relatively high at 400 °C as compared to other operating conditions, the effect of thermal history is only on the devolatilisation process, therefore it may be either due to diffusivity of bed, or when the Fournier number is very high, or increasing residence time of volatile in the matrix accelerates the autocatalytic reactions.

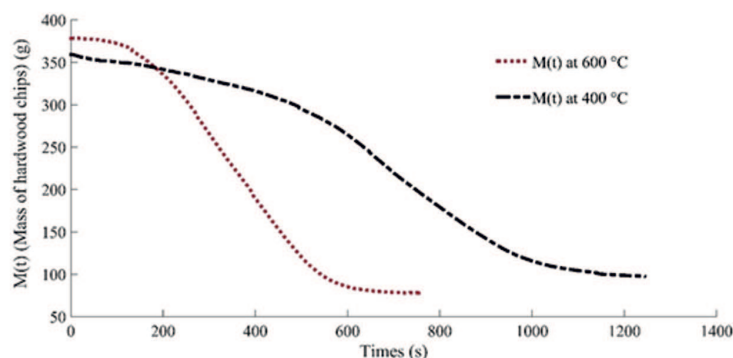


Figure 5: Thermogravimetric variation of hardwood chips at different operating condition.

The variation of thermal efficiency with respect to the height of the reactor is illustrated in Fig. 6. The phenomenal change in the enthalpy of gas is shown in Fig. 7. As it is clearly visible, the operating condition is not a mere factor to decide the overall performance of the reactor. Having seen the optimised operational condition, it inferred that the thermal efficiency of the reactor is not the only function of temperature, but also gas dynamic and heat transfer rate of the system somehow influence it.

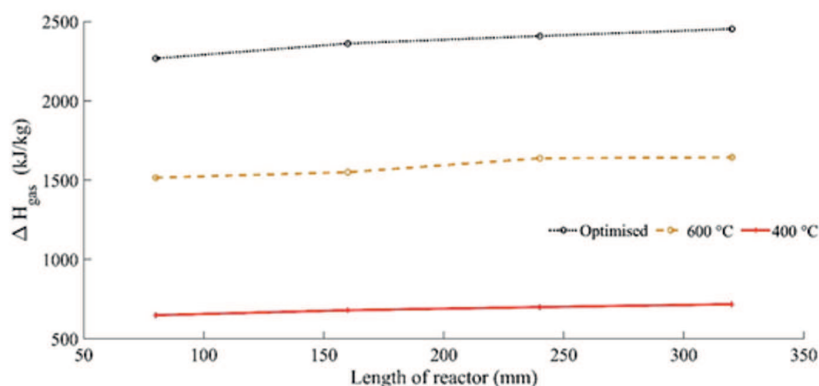


Figure 6: Effect of operating condition on the thermal efficiency.

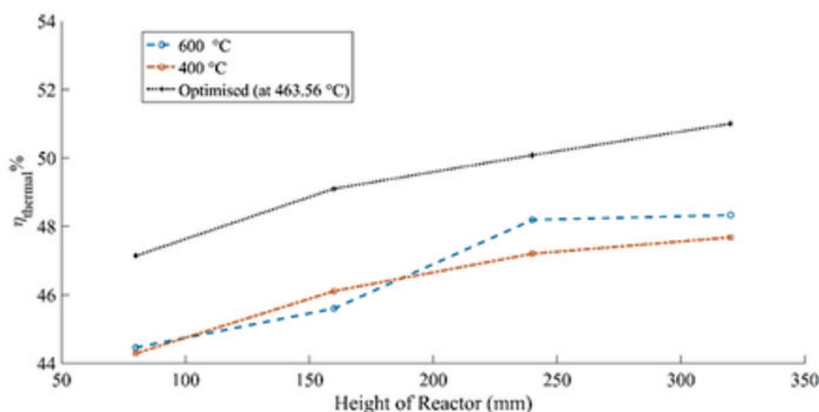


Figure 7: Effect of operating condition on the enthalpy of the gas.

4 Conclusion

The objective of optimising the performance of a unit is successfully achieved via the linear and the nonlinear constraint programming. The overall thermal efficiency of the system has improved by 7%, whereas the enthalpy of formation of gas has found to be 2372.50 kJ/kg, which is 49% higher than enthalpies obtained at different operating conditions. The carbon conversion efficiency of the plant is increased by 1%. The gas yield of the thermal system is edified by 5%. The overall heat loss of plant is minimised by 5%. To prevent excessive pressure drop due to slugging or bubbling of the bed, the gas flow rate must be regulated within permissible limits, which is also

necessary to minimise the entropy generation due to attrition of a solid particle. The temperature near the base of the reactor should not drastically vary with time. The external heat transfer rate must be improved to maximise the utilisation of the external energy supply. The Biot number has shown that the rate of thermochemical conversion relies largely on the external heat transfer. The temperature gradient across the intraparticle is negligible, so there is a possibility of obtaining the efficient carbonised output.

Received 10 May 2019

References

- [1] MOHAN D., PITTMAN C.U., STEELE P.H.: *Pyrolysis of wood/biomass for bio-oil: A critical review*. Energy Fuels **20**(2006), 3, 848–889. DOI: 10.1021/ef0502397
- [2] XU C. ET AL.: *Energy and exergy analysis of solar power tower plants*. Appl. Therm. Eng. **31**(2011), 17–18, 3904–3913. DOI: 10.1016/j.applthermaleng.2011.07.038
- [3] BRIDGWATER A.V., EVANS G.D.: *An assessment of thermochemical conversion systems for processing biomass and refuse*. Rep. ETSU B/T1/00207, 1993.
- [4] DHAUNDIYAL A., GUPTA V.K.: *The analysis of pine needles as a substrate for gasification*. J. Water Energ. Environ. **15**(2014), 73–81. DOI:10.3126/hn.v15i0.11299
- [5] ANTAL M.J. ET AL.: *Review of methods for improving the yield of charcoal from biomass*. Energy Fuels **4**(1990), 3, 221–225. DOI: 10.1021/ef00021a001
- [6] CHAIWAT W. ET AL.: *Examination of degree of cross-linking for cellulose precursors pretreated with acid/hot water at low temperature*. Ind. Eng. Chem. Res. **47**(2008), 16, 5948–5956, DOI: 10.1021/ie800080u
- [7] SIERRA R. ET AL.: *Producing fuels and chemicals from lignocellulosic biomass*. Chem. Eng. Prog. **104**(2008), 8, S10–S18.
- [8] GRAHAM R. ET AL.: *The role of temperature in the fast pyrolysis of cellulose and wood*. Ind. Eng. Chem. Res. **27**(2005), 1, 8–15. DOI: 10.1021/ie00073a003
- [9] RICKY CHAN W. C., KELBON M., KRIEGER-BROCKETT B.: *Single-particle biomass pyrolysis: Correlations of reaction products with process conditions*. Ind. Eng. Chem. Res. **27**(1988), 12, 2261–2275. DOI: 10.1021/ie00084a012
- [10] KUNG H.C.: *A mathematical model of wood pyrolysis*. Combust. Flame **18**(1972), 2, 185–195. DOI: 10.1016/S0010-2180(72)80134-2
- [11] MAA P.S., BAILIE R.C.: *Influence of particle sizes and environmental conditions on high temperature pyrolysis of cellulosic material — I (Theoretical)*. Combust. Sci. Technol. **7**(1973), 6, 257–269. DOI: 10.1080/00102207308952366
- [12] PYLE D.L., ZAROR C.A.: *Heat transfer and kinetics in the low temperature pyrolysis of solids*. Chem. Eng. Sci. **39**(1984), 1, 147–158. DOI: 10.1016/0009-2509(84)80140-2

- [13] KOTHARI V., ANTAL M.J.: *Numerical studies of the flash pyrolysis of cellulose*. *Fuel* **64**(1985), 11, 1487–1494. DOI: 10.1016/0016-2361(85)90361-8
- [14] SIMMONS G.M., GENTRY M.: *Particle size limitations due to heat transfer in determining pyrolysis kinetics of biomass*. *J. Anal. Appl. Pyrol.* **10**(1986), 2, 117–127. DOI: 10.1016/0165-2370(86)85011-2
- [15] DEMIRBAS A.: *Combustion characteristics of different biomass fuels*. *Prog. Energ. Combust. Sci.* (2004), 219–230. DOI: 10.1016/j.pecs.2003.10.004
- [16] MORAN M.J., SCIUBBA E.: *Exergy Analysis: Principles and Practice*. *J. Eng. Gas Turb. Power* **116**(2008), 2, 285–290. DOI: 10.1115/1.2906818
- [17] KOTAS T.J.: *Exergy analysis of simple processes*. In: *The Exergy Method of Thermal Plant Analysis*, Krieger 1995, 99–161. DOI: 10.1016/b978-0-408-01350-5.50011-8
- [18] WALL G., GONG M.: *Exergy analysis versus pinch technology*. In: *Efficiency, Costs, Optimization, Simulation and Environmental Aspects of Energy Systems* (P. Alvfors, Ed.). Royal Institute of Technology, Stockholm 1996, 451–455.
- [19] MCILVRIED H.G. ET AL.: *Exergy and pinch analysis of an advanced ammonia-water coal-fired power cycle*. In: *American Society of Mechanical Engineers, Advanced Energy Systems Division*. *AES* **38**(1998), 197–199.
- [20] HABIB M.A., ZUBAIR S.M.: *Second-law-based thermodynamic analysis of regenerative-reheat Rankine-cycle power plants*. *Energy* **17**(1992), 3, 295–301. DOI: 10.1016/0360-5442(92)90057-7
- [21] HORLOCK J.H., YOUNG J.B., MANFRIDA G.: *Exergy analysis of modern fossil-fuel power plants*. *J. Eng. Gas Turb. Power* **122**(2002), 1, 1–7. DOI: 10.1115/1.483170
- [22] NISHIO M. ET AL.: *A thermodynamic approach to steam-power system design*. *Ind. Eng. Chem. Process Des. Dev.* **19**(1980), 2, 306–312. DOI: 10.1021/i260074a019
- [23] GRIMALDI C.N., BIDINI G.: *Using exergy analyses on circulating fluidized bed combustors*. In: *Proc. A Future for Energy, Florence World Energy Res. Symp.*, Firenze, 1990, 181–19.
- [24] KWAK H.Y., KIM D.J., JEON J.S.: *Energetic and thermoeconomic analyses of power plants*. *Energy* **28**(2003), 4, 343–360. DOI: 10.1016/S0360-5442(02)00138-X
- [25] JIN H. ET AL.: *Exergy evaluation of two current advanced power plants: Supercritical steam turbine and combined cycle*. *J. Energ. Resour. Technol.* **119**(2008), 4, 250–256. DOI: 10.1115/1.2794998
- [26] SILVESTRI G.J., BANNISTER R.L., FUJIKAWA T., HIZUME A.: *Optimization of advanced steam condition power plants*. *J. Eng. Gas Turb. Power* **114**(1992), 612–620.
- [27] GHETTI P. ET AL.: *Coal combustion. Correlation between surface area and thermogravimetric analysis data*. *Fuel* **64**(1985), 7, 950–955. DOI: 10.1016/0016-2361(85)90150-4
- [28] GHETTI P.: *DTG combustion behaviour of coal. Correlations with proximate and ultimate analysis data*. *Fuel* **65**(1986), 5, 636–639. DOI: 10.1016/0016-2361(86)90356-X
- [29] TARTARELLI R. ET AL.: *DTG combustion behaviour of charcoals*. *Fuel* **66**(1987), 12, 1737–1738. DOI: 10.1016/0016-2361(87)90373-5

-
- [30] NAG P.K.: *Power Plant Engineering* (IIIrd Edn.). 2002. DOI: 10.1007/978-1-4613-0427-2.
- [31] HOLMAN J.P.: *Heat Transfer* (10th Edn.). The McGraw-Hill Companies 2010. DOI: 10.1603/EN11245
- [32] LEWELLEN P.C., PETERS W.A., HOWARD J.B.: *Cellulose pyrolysis kinetics and char formation mechanism*. Symp. (Int.) Combust. **16**(1977), 1, 1471–1480. DOI: 10.1016/S0082-0784(??)80429-3
- [33] SLOPIECKA K., BARTOCCI P., FANTOZZI F.: *Thermogravimetric analysis and kinetic study of poplar wood pyrolysis*. Appl. Energ. **97**(2012), 491–497. DOI: 10.1016/j.apenergy.2011.12
- [34] PATEL S.S., LANJEWAR A.: *Exergy based analysis of solar air heater duct with W-shaped rib roughness on the absorber plate*. Arch. Thermodyn. **40**2019, 4, 21–48. DOI: 10.24425/ather.2019.130006